

## DETECTION OF COLLAPSED BUILDINGS DUE TO EARTHQUAKES USING A DIGITAL SURFACE MODEL CONSTRUCTED FROM AERIAL IMAGES

YOSHIHISA MARUYAMA\*, AKIRA TASHIRO  
and FUMIO YAMAZAKI

*Department of Urban Environment Systems  
Chiba University, 1-33 Yayoi-cho  
Inage-ku, Chiba 263-8522, Japan  
\*ymaruyam@tu.chiba-u.ac.jp*

Received 14 December 2011

Accepted 5 January 2013

Published 13 January 2014

The buildings that collapsed during the 2007 Niigata Chuetsu-oki earthquake are detected based on aerial photogrammetry using digital aerial images. The digital surface models (DSMs) in the area where severe damage to buildings was observed after the earthquake are constructed using digital aerial camera images. Pre- and post-event aerial images are employed to obtain the DSMs in this study. The differences in building heights between the pre- and post-event models are considered to detect collapsed buildings and the accuracy of the method is discussed in this paper. The results indicate that the collapsed buildings can be detected and undamaged buildings can also be correctly recognized by the proposed method.

*Keywords:* Digital surface model; aerial photogrammetry; collapsed building.

### 1. Introduction

Remotely sensed data obtained from satellites and airborne platforms are useful in providing understanding of the distribution of damage due to natural disasters [Yamazaki, 2001]. Remote-sensing platforms and sensors should be selected with regards to the coverage and resolution required as well as urgency, weather, and time conditions.

Recently, the use of the digital aerial imaging system has become widespread [Hinz, 1999; Leberl and Gruber, 2005]. The imaging system saves the time associated with analog imagery processes and provides more precise and better-quality aerial images. In addition, the exterior orientations of airborne images can be determined by integrating the global positioning system (GPS) and inertial measurement unit (IMU) observations made during the mapping flight [Grejner-Brzezinska, 1999]. Hence, it is expected that the digital surface model (DSM) can be constructed with good accuracy using the images captured by the imaging system [Zebedin *et al.*, 2006].

Recent advancements in remote sensing technologies and its applications have made it possible to use remotely sensed imagery to estimate the damage distribution due to natural disasters [Rathje and Adams, 2008; Eguchi *et al.*, 2008]. Mitomi *et al.* [2001] attempted to reveal building debris automatically using images captured by a high-definition television camera. Saito *et al.* [2004] performed visual damage inspection using a post-event IKONOS image, in which individual buildings can be identified, and other pre-event satellite images for the 2001 earthquake in Gujarat, India. QuickBird images with a maximum spatial resolution of 0.6 m were also employed to detect collapsed buildings after the 2003 earthquake in Bam, Iran [Yamazaki *et al.*, 2005].

Thus far, remotely sensed images have been effective in detecting earthquake-induced damages. Because we can only obtain the top view of the affected area, some of the damaged buildings are difficult to reveal. Figure 1 depicts an example of the aerial image captured after the 2007 Niigata Chuetsu-oki earthquake. A two-story building with a collapsed first story was identified from the field photo. The building could not be identified from the aerial image because no significant damage was observed on its roof. In this regard, information on building height will play an important role. High-resolution satellite images were employed to update building inventory data by estimating the number of floors with the aid of shadow length [Miura and Midorikawa, 2006]. Pictometric images are built up from aerial images taken in sequence and in different directions from an aircraft. The images not only have a higher resolution but also offer three-dimensional (3D) depth perception; they were used for damage assessment after the 2010 Haiti earthquake [Madabhushi *et al.*, 2011]. Synthetic aperture radar (SAR) satellite data is used for the estimation of building height [Gamba *et al.*, 2000]. The use of building height estimated using SAR images to detect earthquake damage has been discussed by Balz and Liao [2010].



Fig. 1. Comparison between (a) the aerial image and (b) the field photo of the two-story building with the collapsed first story after the 2007 Niigata Chuetsu-oki earthquake.

This study employs a DSM constructed from digital aerial images to reveal the differences of building heights between pre- and post-event models. Aerial photogrammetry is performed on the digital aerial images captured before and after the 2007 Niigata Chuetsu-oki earthquake in Kashiwazaki city, Niigata, Japan. The accuracy of this method is discussed in comparison with the result of visual damage inspection.

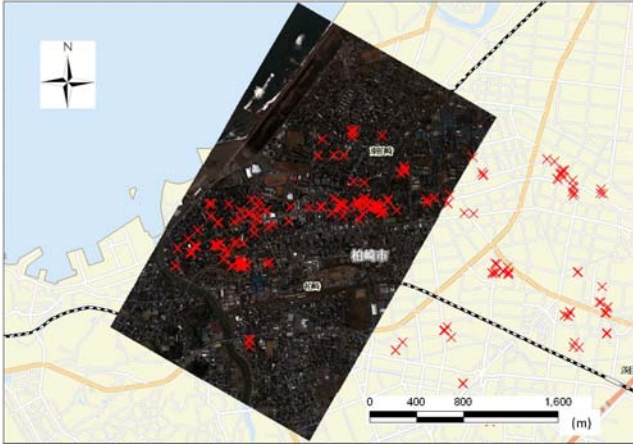
## **2. Construction of the 3D Model for Buildings Using the Pre-Event Aerial Image**

The Niigata Chuetsu-oki earthquake occurred on July 16, 2007 with a Japan Meteorological Agency (JMA) magnitude of 6.8 and a moment magnitude of 6.6 [United States Geological Survey, 2007]. Severe ground shaking was observed near the epicenter and a JMA seismic intensity of 6+ was recorded in Kashiwazaki city, Niigata, Japan [Aoi *et al.*, 2008]. The number of totally collapsed buildings was 1331 and the number of casualties was 15 in the affected area.

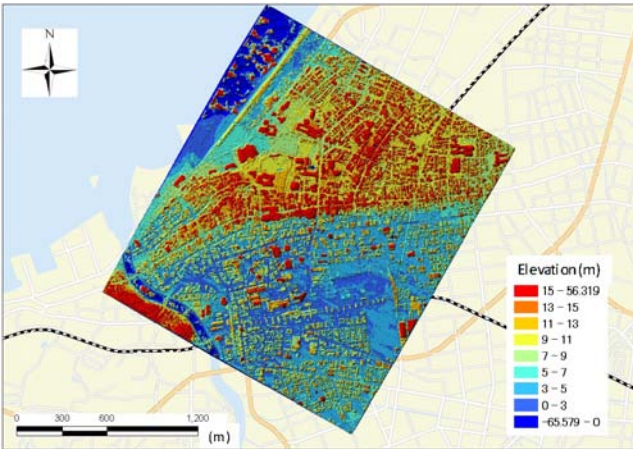
The pre-event digital aerial image was captured for Kashiwazaki city on April 27, 2007, approximately three months before the earthquake. A digital aerial camera, UltraCamD [Leberl and Gruber, 2005], was employed to obtain the aerial images. The effectiveness of UltraCamD images on the detection of affected buildings was discussed by Liu *et al.* [2010] and they presented an automatic change detection method using UltraCamD images and existing 3D CAD data. The UltraCamD provided more precise and better-quality aerial images to detect moving vehicles [Yamazaki *et al.*, 2008a]. The operated digital airborne imaging system was integrated with in-flight control systems consisting of GPS and IMUs. The altitude of the aircraft during image capturing was approximately 1970 m. The spatial resolution of the aerial images is 0.17 m.

The exterior orientation parameters are required to establish the location of the aerial image in terms of map projections. The exterior orientation parameters are defined by the position and the orientation of the camera at the moment of exposure. In photogrammetry, the six exterior orientation parameters (three coordinates of the perspective center and three rotational angles) are determined using a mathematical model for transformation between object and image spaces, defining the correlation between ground control points and their corresponding image representations [Grejner-Brzezinska, 1999; Habib *et al.*, 2000]. Collinearity equations provide an essential basis for photogrammetry applications in which the observables in the image and object spaces are related within an imaging system. Various algorithms for determining the orientation parameters were recently proposed [Hati and Sengupta, 2001; Nakano and Chikatsu, 2010; Han *et al.*, 2011].

If the position and the orientation of aircraft are monitored by GPS and IMU during flight, the exterior orientation parameters are directly obtained. For the pre-event images, five sheets of aerial images are established in a map coordinate system and stereo-pairs of digital aerial images are created (Fig. 2(a)). DSMs are



(a)



(b)

Fig. 2. (Color online) (a) Stereo-pairs of pre-event aerial images and (b) the DSM obtained through aerial photogrammetry. The x-marks in Fig. 2(a) indicate the locations of collapsed buildings due to the earthquake detected by Geospatial Information Authority of Japan.

standard products in aerial photography that employ analytical and digital photogrammetric techniques. Analytical photogrammetry is a well-established mapping technique that can provide reliable and accurate measurements [Smith *et al.*, 2004]. Figure 2(b) shows the DSM estimated from the pre-event images through aerial photogrammetry.

The DSM illustrated in Fig. 2(b) was computed on the basis of aerial photogrammetry. It is difficult to construct a 3D model of buildings solely from the computed DSM. Hence, the breaklines [Briese, 2004], which describe the discontinuities of the elevations and are basically extracted manually, were considered in the pre-event

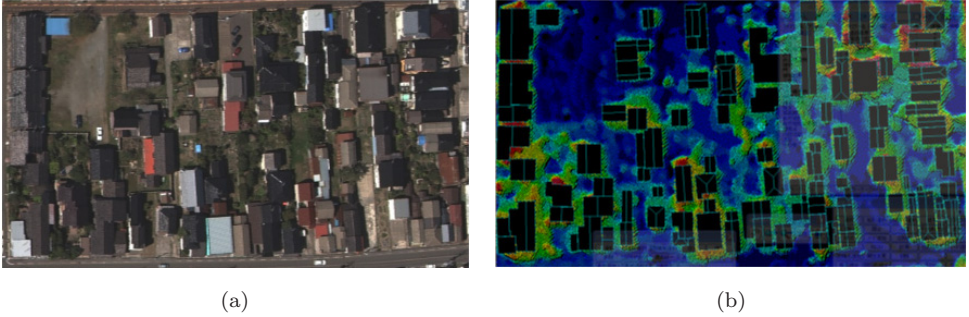


Fig. 3. (Color online) Consideration of breaklines extracted from (a) the digital aerial image in (b) the computed DSM.

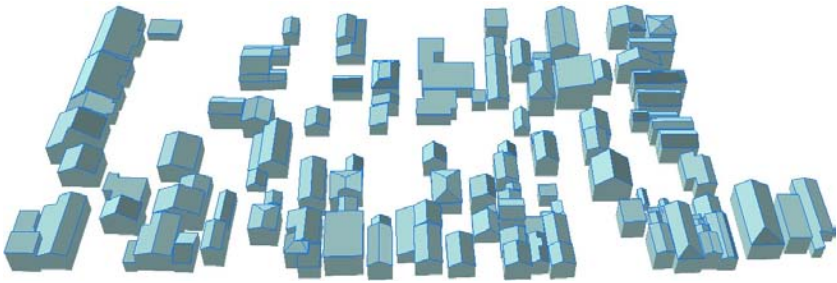


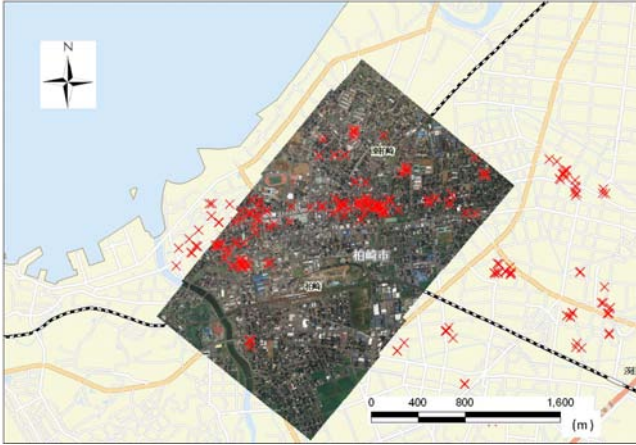
Fig. 4. The 3D model for buildings constructed from the pre-event images.

DSM (Fig. 3). After the elevations were assigned to both ends of the breaklines, the 3D model of the buildings was eventually created based on the stereo-pairs of pre-event aerial images (Fig. 4). One hundred and nine buildings are realized in the 3D model, which took approximately 2 h to generate.

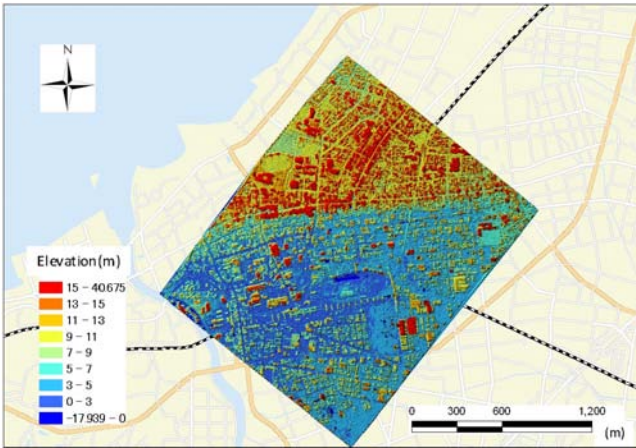
### **3. Construction of the DSM Using the Post-Event Aerial Images**

The post-event digital aerial images were captured by Asia Air Survey Co. Ltd. on July 19, 2007 (three days after the earthquake). A digital mapping camera system (DMC) was employed to obtain the aerial images in the affected areas. The GPS/IMU system was also operated during the flight. Following the same procedure as the previous chapter, six sheets of aerial images were established in terms of map projection using the record of the GPS/IMU system and stereo-pairs of images were developed (Fig. 5(a)). Next, aerial photogrammetry was performed to compute the DSM from the post-event aerial images.

In general, differential GPS is employed during the mapping flight to determine the precise position of the airborne image [Light, 2001]. Differential GPS requires a GPS receiver to be established at a fixed point for which the geographic location is known [Campbell, 2006]. The Geospatial Information Authority of Japan (GSI)



(a)



(b)

Fig. 5. (Color online) (a) Stereo-pairs of post-event aerial images and (b) the DSM. The x-marks in Fig. 5(a) indicate the locations of collapsed buildings due to the earthquake detected by Geospatial Information Authority of Japan. The exterior orientations were determined by the locations of ground control points extracted from pre-event images to construct the post-event DSM (see Fig. 6).

has established approximately 1200 GPS-based control stations throughout Japan [GSI, 2011]. Using the signal from the ground-based reference stations, the accurate location can be determined by differential GPS. In the case of a large earthquake, the stations are not activated because their locations might be changed because of the effects of crustal movements. The GPS-based control stations in Kashiwazaki were stopped after the Niigata Chuetsu-oki earthquake; they restarted on August 17, 2007 [GSI, 2007].

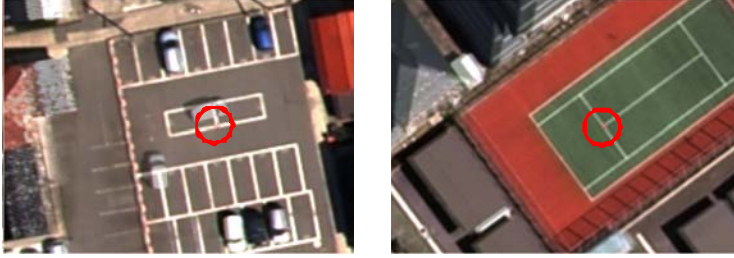


Fig. 6. Extraction of control points from the stereo-pairs of pre-event images to revise those of post-event images.

As mentioned above, the record of the GPS/IMU system of the post-event aerial images is not adjusted by the signal of the GPS-based control stations. The accuracy of positioning is not high enough to perform aerial photogrammetry. Although the DSM could be computed from the post-event images, the DSM from the post-event images obviously showed fewer elevations and horizontal deformations. This study attempts to detect the collapsed buildings based on the differences in building height between the pre- and post-event DSMs. To achieve the objective, the DSM constructed from the post-event images should be correctly adjusted.

In this study, the stereo-pairs of post-event aerial images were re-established in terms of map coordinates by introducing ground control points. The ground control points were extracted from the stereo-pairs of pre-event images because they could be georeferenced correctly with the record of the GPS/IMU system. Figure 6 shows examples of the control points extracted from the stereo-pair of the pre-event images. A total of 12 control points were extracted from the pre-event images. Assuming a collinearity condition [Habib *et al.*, 2000], the exterior orientations of the post-event images were calculated based on the locations of the 12 control points. Then, the computational DSM was developed from the post-event images (Fig. 5(b)).

#### 4. Detection of Collapsed Buildings Due to the Earthquake

The differences in building height are employed to detect collapsed buildings due to the earthquake. The triangulated irregular network (TIN) generated from the 3D model for the buildings shown in Fig. 4 is used to determine the heights of the buildings before the event. It takes more time to construct the 3D model of the buildings than to compute the DSM because the breaklines that can be extracted manually are required to develop the 3D model. However, we have a preparation period to make the 3D model of buildings before the event and some of the 3D GIS datasets [Zhou *et al.*, 2004] with building height have recently been well developed. Considering these situations, the authors assume that detailed information on building height can be prepared before an earthquake and the 3D model of buildings in Fig. 4 is used to reveal the building height before the event.

For the post-event images, the height of buildings was estimated in two ways. Because grasping building damage in a labor- and time-efficient manner in the early stage of an earthquake is desired, immediacy was prioritized by using the computed DSM. The DSM can be developed numerically if several ground control points to make stereo-pairs of post-event aerial images are prepared. Although the computed DSM cannot represent the clear outlines of buildings, it is expected to be able to grasp the height of buildings in an early stage of an earthquake. To evaluate the accuracy of damage detection, a 3D model of buildings with the aid of breaklines was also constructed from the post-event images. The building heights after the earthquake could be estimated more precisely using the 3D model from the breaklines.

Subtracting the height of the building estimated from the post-event images from that of the pre-event model, the collapsed buildings were extracted. According to Hobi and Ginzler [2012], the vertical median error of the DSM constructed from images captured by a digital aerial imaging system is less than 4.8 times of spatial resolution, which corresponds to approximately 0.8 m in this study. Hence, the DSMs developed from the aerial images can be used for accurate height modeling. Since this study tries to detect buildings with a collapsed first story, the threshold value to detect this failure mode is set to be 2.5 m. In this regard, the authors assume that the average height of each story is approximately 3 m. Figure 7 shows the results of the detection of collapsed buildings, taking into consideration the differences in heights between the pre- and post-event models. Since the detailed damage information of buildings was difficult to access, the accuracy of the estimation was examined through comparison with the result of the visual damage inspection of the aerial image and field photos shown in Fig. 8. Table 1 summarizes the comparisons. Here, partial collapse refers to buildings whose less than half of areas are covered with red pixels in Fig. 7. An inclined building was found through the visual damage inspection of field photos in the lower part of Fig. 8 and it was also labeled as partially collapsed in Table 1.

According to the visual inspection, 18 collapsed, 1 partially collapsed, and 90 undamaged buildings were observed. When the height of buildings was estimated from the computed DSM, 16 of the 18 collapsed buildings could be pointed out. Although the 13 undamaged buildings were misrecognized as collapsed ones, these are located in the upper-right area of Fig. 7(a), where the computed DSM contained much noise. Because of the less accurate DSM, some of the buildings were mistakenly recognized as being collapsed. Except for this area, many of the undamaged buildings were correctly detected using the computed post-event DSM. Using the height of buildings estimated by the 3D model that considered breaklines, only 5 of the 109 buildings were incorrectly detected. This result suggests that better estimations could be obtained if detailed information regarding building height is available after an earthquake.

Various studies are performed to detect damage to buildings after the earthquake using remotely sensed imageries. Pixel- and object-based classifications were



(a)



(b)

Fig. 7. (Color online) Results of detection of collapsed buildings considering the differences in building height between the pre- and post-event models. The height of buildings after the earthquake was estimated from (a) the computed DSM and (b) the 3D model constructed using breaklines. Red pixels indicate those with height differences of more than 2.5 m.

Table 1. Comparisons of the number of buildings with respect to the damage level estimated using aerial images.

Source of post-event building height	Damage level	Visual damage inspection (Fig. 8)			Total
		No damage	Partial collapse	Collapse	
Computed DSM (Fig. 7(a))	No damage	66	0	2	69
	Partial collapse	11	0	1	12
	Collapse	13	1	15	29
	Total	90	1	18	109
3D model considering breaklines (Fig. 7(b))	No damage	86	0	0	86
	Partial collapse	4	1	1	6
	Collapse	0	0	17	17
	Total	90	1	18	109



Fig. 8. (Color online) Examples of visual damage inspection using aerial images and field photos and detected collapsed buildings by this study.

performed to detect damage to buildings after the 2007 Niigata Chuetsu-oki earthquake [Yamazaki *et al.*, 2008b]. It will give better estimations to consider both the changes of imagery texture and those of building height. To develop an urban 3D model, various sensors and platforms (e.g. light detection and ranging [LiDAR]), have recently been employed [Zhou *et al.*, 2004; Vu *et al.*, 2009]. The accuracy of damage detection performed in this study can be examined in detail if the imageries obtained from these sensors and platforms are available.

## 5. Conclusions

This study constructed DSMs using aerial images captured by a digital airborne imaging system integrated with in-flight control systems consisting of GPS and IMUs. Based on the differences in building height estimated from the pre- and post-event aerial images, the buildings that collapsed as a result of the 2007 Niigata Chuetsu-oki earthquake were detected.

After a damage-inducing earthquake, the GPS-based control points are affected by crustal movements and they are difficult to be used in the adjustment of

GPS/IMU aviation data. Although the post-event DSM could be computed in the automated method, it obviously showed fewer elevations and horizontal deformations. In order to modify the post-event DSM, the exterior orientations were re-established in terms of map projection based on the locations of the 12 control points settled from the stereo-pairs of the pre-event images. The revised DSM after the earthquake could subsequently be obtained.

Considering the differences in building height between the pre- and post-event models, the collapsed buildings were detected in this study. We assume that there is a preparation period before the earthquake to construct the 3D model of buildings with the aid of breaklines that can be set manually. In terms of the building height after the earthquake, the computed DSM was employed under the condition that immediacy was prioritized. Both the collapsed and undamaged buildings were correctly detected except for the area, where the DSM contained a great deal of noise. It is expected that more accurate estimations could be obtained if the 3D model of buildings that takes breaklines into consideration is prepared after an earthquake.

These results indicate that 3D information will play an important role in detecting collapsed or partially collapsed buildings.

## **Acknowledgments**

The authors would like to express their sincere gratitude to the Kashiwazaki city government and Asia Air Survey Co. Ltd. for providing the digital aerial images.

## **References**

- Aoi, S., Sekiguchi, H., Morikawa, N. and Kunugi, T. [2008] "Source process of the 2007 Niigata-ken Chuetsu-oki earthquake derived from near-fault strong motion data," *Earth Planets Space* **60**, 1131–1135.
- Balz, T. and Liao, M. [2010] "Building-damage detection using post-seismic high-resolution SAR satellite data," *Int. J. Remote Sens.* **31**(13), 3369–3391.
- Briese, C. [2004] "Three-dimensional modelling of breaklines from airborne laser scanner data," *International Archives of the Photogrammetry, Remote Sensing and Spatial Information Sciences* **35**, 1097–1102.
- Campbell, J. B. [2006] *Introduction to Remote Sensing* (Taylor & Francis, New York).
- Eguchi, R. T., Huyck, C. K., Ghosh, S. and Adams, B. J. [2008] "The application of remote sensing technologies for disaster management," *Proc. 14th World Conf. Earthquake Engineering*, Paper ID. K004, 17 pp.
- Gamba, P., Houshmand, B. and Saccani, M. [2000] "Detection and extraction of buildings from interferometric SAR data," *IEEE Trans. Geosci. Remote Sens.* **38**, 611–618.
- Geospatial Information Authority of Japan (GSI) [2011] "Geodetic survey," Available at [http://www.gsi.go.jp/ENGLISH/page\\_e30030.html](http://www.gsi.go.jp/ENGLISH/page_e30030.html), last accessed on 1 December 2011.
- Geospatial Information Authority of Japan (GSI) [2007] Available at <http://www.gsi.go.jp/1SEIKA/h19nigata-seika.html> (in Japanese), last accessed on 1 December 2011.
- Grejner-Brzezinska, D. A. [1999] "Direct exterior orientation of airborne imagery with GPS/INS system: Performance analysis," *Navigation* **46**(4), 261–270.

- Habib, A., Asmamaw, A., Kelly, D. and May, M. [2000] “Linear features in photogrammetry,” *Geodetic science and surveying*, Department of Civil and Environment Engineering and Geodetic Science, The Ohio State University. It is available at [http://www.geology.osu.edu/~jekeli.1/OSUReports/reports/report\\_450.pdf](http://www.geology.osu.edu/~jekeli.1/OSUReports/reports/report_450.pdf), last accessed on 23 December, 2013.
- Han, J. Y., Guo, J. and Chou, J. Y. [2011] “A direct determination of the orientation parameters in the collinearity equations,” *IEEE Geosci. Remote Sens. Lett.* **8**(2), 313–316.
- Hati, S. and Sengupta, S. [2001] “Robust camera parameter estimation using genetic algorithm,” *Pattern. Recogn. Lett.* **22**(3–4), 289–298.
- Hinz, A. [1999] “The Z/I digital aerial camera system,” *Proc. 47th Photogrammetric Week 1999*, pp. 109–115.
- Hobi, M. L. and Ginzler, C. [2012] “Accuracy assessment of digital surface models based on WorldView-2 and ADS80 stereo remote sensing data,” *Sensors* **12**, 6347–6368.
- Leberl, F. and Gruber, M. [2005] “ULTRACAM-D: Understanding some noteworthy capabilities,” *Proc. 53th Photogrammetric Week 05*, pp. 57–68.
- Light, D. [2001] “An airborne direct digital imaging system,” *Photogramm. Eng. Remote Sens.* **67**(11), 1299–1305.
- Liu, Z., Gong, P., Shi, P., Chen, H., Zhu, L. and Sasagawa, T. [2010] “Automated building change detection using UltraCamD images and existing CAD data,” *Int. J. Remote Sens.* **31**(6), 1505–1517.
- Madabhushi, S. P. G., Saito, K. and Booth, E. [2011] “Post-earthquake field mission to Haiti,” *Proc. Ninth Pacific Conf. Earthquake Engineering*, Paper No. 183, 8 pp.
- Mitomi, H., Yamazaki, F. and Matsuoka, M. [2001] “Development of automated extraction method for building damage area based on maximum likelihood classifier,” *Proc. 8th Int. Conf. Structural Safety and Reliability*, CD-ROM, 8 pp.
- Miura, H. and Midorikawa, S. [2006] “Updating GIS building inventory data using high-resolution satellite images for earthquake damage assessment: Application to Metro Manila, Philippines,” *Earthq. Spectra* **22**(1), 151–168.
- Nakano, K. and Chikatsu, H. [2010] “Camera calibration techniques using multiple cameras of different resolutions and bundle of distances,” *Proc. ISPRS Commission V Mid-Term Symp. ‘Close Range Image Measurement Techniques’*, Vol. XXXVIII — Part 5, pp. 484–489.
- Rathje, E. M. and Adams, B. J. [2008] “The role of remote sensing in earthquake science and engineering: Opportunities and challenges,” *Earthq. Spectra* **24**(2), 471–492.
- Saito, K., Spence, R., Going, C. and Markus, M. [2004] “Using high-resolution satellite images for post-earthquake building damage assessment: A study following the 26 January 2001 Gujarat earthquake,” *Earthq. Spectra* **20**(1), 145–169.
- Smith, M. J., Asal, F. F. F. and Priestnall, G. [2004] “The use of photogrammetry and LIDAR for landscape roughness estimation in hydrodynamic studies,” *Proc. Int. Society for Photogrammetry and Remote Sensing XXth Congress*, Vol. XXXV, WG III/8, p. 6.
- United States Geological Survey [2007] Available at <http://earthquake.usgs.gov/earthquakes/eqinthenews/2007/us2007ewac/#details>, last accessed on 1 December, 2011.
- Yamazaki, F. [2001] “Applications of remote sensing and GIS for damage assessment,” *Proc. 8th Int. Conf. Structural Safety and Reliability*, CD-ROM, 12 pp.
- Yamazaki, F., Yano, Y. and Matsuoka, M. [2005] “Visual damage interpretation of buildings in Bam city using QuickBird images following the 2003 Bam, Iran, Earthquake,” *Earthq. Spectra* **21**(S1), 329–336.

- Yamazaki, F., Liu, W. and Vu, T. T. [2008a] “Vehicle extraction and speed detection from digital aerial images,” *Proc. IEEE 2008 Int. Geoscience and Remote Sensing Symp. IEEE*, CD-ROM, 4 pp.
- Yamazaki, F., Suzuki, D. and Maruyama, Y. [2008b] “Use of digital aerial images to detect damages due to earthquakes,” *Proc. 14th World Conf. Earthquake Engineering*, Paper No. 01-1049, CD-ROM, 8 pp.
- Vu, T. T., Yamazaki, F. and Matsuoka, M. [2009] “Multi-scale solution for building extraction from LiDAR and image data,” *Int. J. Appl. Earth Obs. Geoinfo.* **11**, 281–289.
- Zebedin, L., Klaus, A., Gruber-Geymayer, B. and Karner, K [2006] “Towards 3D map generation from digital aerial images,” *ISPRS J. Photogramm. Remote Sens.* **60**, 413–427.
- Zhou, G., Songa, C., Simmers, J. and Cheng, P. [2004] “Urban 3D GIS from LiDAR and digital aerial images,” *Comput. Geosci.* **30**, 345–353.